## Research Article
# Channel Asymmetry in Cellular OFDMA-TDD Networks

**Ellina Foutekova,[1] Patrick Agyapong,[2, 3] and Harald Haas[1]**

[1] *Institute for Digital Communications, School of Engineering & Electronics, The University of Edinburgh, Edinburgh, EH9 3JL, UK*
[2] *School of Engineering and Science, Jacobs University Bremen, 28759 Bremen, Germany*
[3] *Department of Engineering and Public Policy, College of Engineering, Carnegie Mellon University, Pittsburgh, PA 15213, USA*

Correspondence should be addressed to Ellina Foutekova, e.foutekova@ed.ac.uk

This paper studies time division duplex- (TDD-) specific interference issues in orthogonal frequency division multiple access- (OFDMA-) TDD cellular networks arising from various uplink (UL)/downlink (DL) traffic asymmetries, considering both line-of-sight (LOS) and non-LOS (NLOS) conditions among base stations (BSs). The study explores aspects both of channel allocation and user scheduling. In particular, a comparison is drawn between the fixed slot allocation (FSA) technique and a dynamic channel allocation (DCA) technique for different UL/DL loads. For the latter, random time slot opposing (RTSO) is assumed due to its simplicity and its low signaling overhead. Both channel allocation techniques do not obviate the need for user scheduling algorithms, therefore, a greedy and a fair scheduling approach are applied to both the RTSO and the FSA. The systems are evaluated based on spectral efficiency, subcarrier utilization, and user outage. The results show that RTSO networks with DL-favored traffic asymmetries outperform FSA networks for all considered metrics and are robust to LOS between BSs. In addition, it is demonstrated that the greedy scheduling algorithm only offers a marginal increase in spectral efficiency as compared to the fair scheduling algorithm, while the latter exhibits up to ≈20% lower outage.

## 1. INTRODUCTION

In the recent years, orthogonal frequency division multiplexing (OFDM) has been a subject of considerable interest for cellular systems of beyond third generation (3G). Wong et al. [1] show promising results for OFDM as a multiuser technique, focusing particularly on the gains in using adaptive modulation. Results, presented by Keller and Hanzo in [2], also highlight the solid benefits of employing adaptive modulation in OFDM systems. Later, Yan et al. [3] propose an adaptive subcarrier, bit, and power allocation algorithm for a multiuser, multicell OFDM system, which shows significant improvement in throughput when compared to an equal power allocation algorithm. Limiting assumptions include frequency reuse of four, no Doppler effect, no own-cell interference. The gains in combining OFDM with an adequate multiple access scheme have been thoroughly described in [4], specifically emphasizing on the superiority of frequency division multiple access (FDMA).

The combination of OFDMA with time division duplex (TDD), which enables the support of asymmetric services, is of special interest [5]. However, in a system where cell-specific asymmetry demands are to be supported, TDD suffers from additional interference as compared to frequency divisionduplex (FDD), namely same-entity interference (base station (BS) → BS and mobile station (MS) → MS). A possible solution to the same-entity interference problem is fixed slot allocation (FSA). The principle of FSA is that the uplink-downlink (UL-DL) time slot assignment ratio is kept fixed and constant across the cells in a network (and usually allocates half of the resources to UL and DL each). FSA is convenient because, most importantly, same-entity interference is completely avoided, and, in addition, the scheme is simple-to-implement and there is no signaling overhead. The major disadvantage, however, is the lack of flexibility. In other words, one of the primary advantages of TDD, namely, the support for cell-specific asymmetry demands is not exploited.

An interference mitigation technique, which retains the advantages of TDD is random time slot opposing (RTSO) [6]. In RTSO, each cell independently sets the number of UL and DL time slots based on the cell-specific traffic
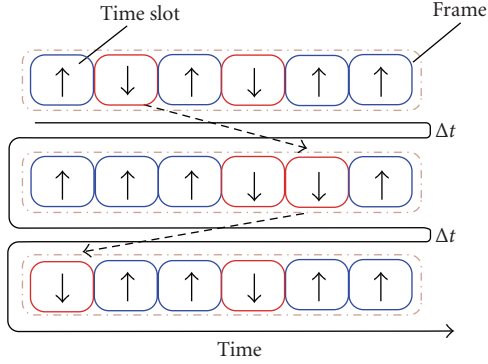
FIGURE 1: For a given ratio of UL/DL resources, RTSO only permutes the UL and DL time slots once every time interval $\Delta t$ (greater than the frame duration) [6], keeping the UL/DL ratio fixed. Upward-pointing arrow denotes UL, while DL is denoted by a downward-pointing arrow.

asymmetry demand. In order to mitigate the same-entity interference problem, the time slots are randomly permuted within a frame once every time interval $\Delta t$ (where $\Delta t$ is a network parameter) as illustrated in Figure 1. The actual time slot permutation sequence follows a pseudorandom pattern. This pattern can be independently generated at both ends (MS and BS). As a consequence, the signaling effort is almost negligible since only a random code at link setup needs to be conveyed. RTSO avoids persistent severe interference, and in effect achieves interference diversity. Note that an analogy can be made between RTSO and frequency hopping. In the latter, interference diversity is achieved by hopping through different frequency carriers. RTSO has been previously applied to code division multiple access (CDMA) systems [6].

The purpose of this paper is to explore interference aspects arising from cell-specific traffic asymmetry demands in OFDMA-TDD cellular networks, while jointly considering channel allocation and user scheduling. A multiuser, multicell OFDMA-TDD network with full-frequency reuse is studied, assuming both LOS and NLOS conditions among the BSs. RTSO and FSA are the considered channel allocation techniques and the two alternative scheduling algorithms are the fair *optimum target assignment with stepwise rate removals* (OTA-SRRs) [7] and the *greedy rate packing* (GRP) [8].

The rest of the paper is organized as follows. Section 2 presents the system model, while the employed scheduling algorithms are described in Section 3. The simulation model and results are given in Sections 4 and 5, respectively. Concluding remarks are presented in Section 6.

## 2. SYSTEM MODEL

A wireless cellular network can be modeled mathematically by the signal-to-interference-plus-noise-ratio (SINR) expression in the sense that the SINR expression holds information about the model assumptions on interference sources and power fading alike. In terms of power fading, the system

model considered in this study takes on a realistic cross-layer approach to reflect both small-scale fading and large-scale fading in a typical time-variant frequency-selective channel. Small-scale fading pertains to the received signal power variations with frequency, while large-scale fading pertains to the received signal power variations with distance [9]. In previous studies [1–4], one of these impairments is usually neglected. However, for cellular OFDM systems with increasing channel bandwidth (100 MHz for beyond 3G networks [10]), it is important that both fading effects are considered due to the frequency selectivity and frequency granularity, introduced by OFDM. In terms of interference sources, this study considers contributions from own-cell links and other-cell links, termed multiple-access interference (MAI) and cochannel interference (CCI), respectively. Furthermore, impairments such as frequency offset errors due to Doppler and lack of synchronization are also accounted for.

In what follows, expressions for the desired signal power per subcarrier, the received MAI power, and the received CCI power are presented, which are then combined to formulate an SINR expression according to the system model described above.

Let subcarrier $k \in \mathbf{s} = \{a_1, \ldots, a_m\}$, where $a_i \in \{1, \ldots, N_c\}$ and $\mathbf{s}$ is a set of subcarriers belonging to a single user in cell $i$, and $k$ does not experience interference from the set. The cardinality of $\mathbf{s}$, $|\mathbf{s}|$, is the number of subcarriers per user, which can vary from zero to $N_c$ (total number of subcarriers per BS). The received signal power on subcarrier $k$ in cell $i$ is given by

$$R_k^i = P_k^i G_k^i |H_k^i|^2 \text{ [W]}, \tag{1}$$

where $P_k^i$ is the transmit power on subcarrier $k$ in cell $i$, $G_k^i$ is the path gain between the MS using subcarrier $k$ and its corresponding BS, and $H_k^i$ is the channel transfer function for subcarrier $k$ in cell $i$ between the MS using subcarrier $k$ and its corresponding BS. Here, it should be noted that the path loss reflects the variation of the received signal power with distance, while the channel transfer function reflects the variation of the received signal power with frequency.

The received MAI power on subcarrier $k$ in UL is given by (2), where it should be noted that MAI in DL is not considered, as perfect synchronization is assumed due to the synchronous nature of point-to-multipoint communication:

$$P_{\text{MAI},k}^i = \sum_{\substack{k'=1 \\ k' \notin \mathbf{s}}}^{N_c} P_{k'}^i G_{k,k'}^i |H_{k,k'}^i|^2 |C_{k,k'}^i(\Delta f + \varepsilon_D + \omega)|^2 \text{ [W]}, \tag{2}$$

where

$$C_{k,k'}^i(x) = \left(\frac{1}{N_c}\right) \frac{\sin(\pi x)}{\sin(\pi x/N_c)} \exp \frac{j\pi x(N_c - 1)}{N_c}, \tag{3}$$

$G_{k,k'}^i$ is the path gain between the transmitter on the link using subcarrier $k'$ and the receiver on the link using subcarrier $k$, $H_{k,k'}^i$ is the transfer function of the channel between the transmitter on the link using subcarrier $k'$ and

the receiver on the link using subcarrier $k$, $C_{k,k'}^i(\Delta f + \varepsilon_D + \omega)$, given in (3), is a cyclic sinc function to account for the amount of interference subcarrier $k$ experiences from subcarrier $k'$, $j$ is the imaginary unit, $\Delta f = k' - k$ and $\varepsilon_D = f_{D,\max}/\delta_f$ accounts for the Doppler shift (where $f_{D,\max}$ is the maximum Doppler frequency and $\delta_f$ is the carrier spacing), $\omega = f_c/\delta_f$ is the frequency offset due to synchronization errors between subcarriers $k$ and $k'$, and $f_c$ is the offset in Hz. A derivation of the cyclic sinc function is presented in Appendix C.

The received CCI power per subcarrier is modeled similarly to the received MAI power and is given by (4), where it should be noted that CCI contributions are expected not only from the reused subcarrier but also from neighboring subcarriers, when $\varepsilon_D$ and/or $\omega$ are non-zero:

$$P_{\mathrm{CCI},k}^i = \sum_{\substack{l=1 \\ l \neq i}}^{B} \sum_{k'=1}^{N_c} P_{k'}^l G_{k,k'}^l |H_{k,k'}^l|^2 |C_{k,k'}^l(\Delta f + \varepsilon_D + \omega)|^2 \; [\mathrm{W}],$$

(4)

where $B$ is the number of cells under consideration (cells that contribute nonnegligible interference).

The cyclic sinc function used in modeling MAI and CCI controls the amount of interference subcarrier $k'$ causes to subcarrier $k$. Given the same transmit power, link gain, and channel, with an increase in $|k' - k + \varepsilon_D + \omega|$, the interference contribution decreases. This behavior is expected as synchronization errors and Doppler effects are significant to neighboring subcarriers and become negligible when the subcarriers are spaced relatively far apart.

Based on (1) through (4), the achieved SINR on subcarrier $k \in \mathbf{s}$ in cell $i$, $\gamma_k^i$, can be written as

$$\gamma_k^i = \frac{P_k^i \widetilde{G}_k^i}{\sum_{l=1}^{B} \sum_{\substack{k'=1 \\ \text{if } l=i, k' \notin \mathbf{s}}}^{N_c} P_{k'}^l \widetilde{G}_{k,k'}^l(\cdot) + n},$$

(5)

where $\widetilde{G}_k^i = G_k^i |H_k^i|^2$ is the weighted gain on the "desired" link for subcarrier $k \in \mathbf{s}$, $\widetilde{G}_{k,k'}^l(\cdot) = G_{k,k'}^l |H_{k,k'}^l|^2 |C_{k,k'}^l(\Delta f + \varepsilon_D + \omega)|^2$ is the weighted gain of the interfering link between the transmitter on the link using subcarrier $k'$ and the receiver on the link using subcarrier $k$, and $n$ is the thermal noise power per subcarrier. As MAI in DL is not considered, in the case of DL SINR calculation when $i = l$ and $k' \notin \mathbf{s}$, $\widetilde{G}_{k,k'}^l(\cdot) = 0$.

It should be noted that this study assumes that adaptive modulation is in place. For each $\gamma_k^i$, $\overline{\gamma}_k$ is assigned, where $\overline{\gamma}_k$ is the target SINR of subcarrier $k$, such that $\overline{\gamma}_k \leq \gamma_k^i$ and $\overline{\gamma}_k \in \{\widetilde{\gamma}_1 < \widetilde{\gamma}_2 < \cdots < \widetilde{\gamma}_m\}$. Furthermore, suppose that a number of $m$ discrete transmission rates are available, $r_k \in \{r_1 < r_2 < \cdots < r_m\}$ depending on the modulation alphabet, where each SINR target element corresponds to each rate, respectively. Employing adaptive modulation, if a subcarrier has high SINR, high data rate for the same bit error ratio (BER) can be maintained on that subcarrier, simply by using a high-order modulation scheme.

## 3. SCHEDULING ALGORITHMS

This section treats the GRP and OTA-SRR scheduling algorithms and their adaptation to OFDMA based on the SINR equation formulated in Section 2.

### 3.1. Modified GRP

GRP is a simple heuristic scheduling algorithm, which formulates the problem of supporting different users with different data rates into a joint power and rate control scheme. GRP allocates high transmission rates to users having high link gains, and hence can be considered a form of water filling. The greedy nature of GRP is exhibited in that the aim is to *maximize throughput* while *minimizing transmit power*. As a result, users with the best link gains are identified and served. Typically, these are the users close to the BS.

An extensive work on GRP for direct sequence CDMA (DS-CDMA) systems is presented in [8], where it was applied to a single cell, using fixed intercell interference. The modified GRP is an iterative algorithm executed by each BS in the network and accounts for both MAI and CCI which are dynamically updated during each iteration. The modified algorithm can be summarized as follows: initially, all subcarriers are assigned maximum available transmit power, then, an iterative procedure begins, where at each iteration step interference is calculated and then the SINR target, power target, and rate target are calculated for all subcarriers and assigned accordingly. Subcarriers which are assigned transmit power higher than the maximum allowed power per subcarrier are blocked. Every single step of the algorithm is first processed by each individual BS before any of the BSs starts processing the subsequent step (pseudoparallel operation). This is repeated until convergence is reached which happens when there are no significant changes (defined as arbitrarily small changes within some interval $\epsilon$) in a feasible SINR target and power target assignment for a series of consecutive iterations. A feasible assignment is an assignment where each assigned SINR target can be achieved while maintaining the maximum power constraint per subcarrier. It should be noted that convergence of the modified GRP algorithm is tested via Monte Carlo simulations, which demonstrate that the algorithm reaches convergence in 50 iterations (not shown). As a safeguard, it is assumed that the algorithm always converges after 100 iterations.

The formulation of the modified GRP utilizes the SINR expression presented in Section 2 and slightly rearranges it to suit the algorithm derivation. Given a vector of powers with elements being the power on each subcarrier, $\mathbf{P} = (P_1, P_2, \ldots, P_{N_c})^T$, the received SINR on subcarrier $k$, is defined by (6) and (7) for UL and DL, respectively:

$$\gamma_{k,\mathrm{UL}} = \frac{P_k G_k |H_k|^2}{\sum_{k'=1, \, k' \notin \mathbf{s}}^{N_c} |S_{k,k'}|^2 |H_{k,k'}|^2 |C_{k,k'}(z)|^2 + P_{\mathrm{CCI},k} + n},$$

(6)

$$\gamma_{k,\mathrm{DL}} = \frac{P_k G_k |H_k|^2}{P_{\mathrm{CCI},k} + n},$$

(7)

where $\gamma_{k,\text{UL}}$ and $\gamma_{k,\text{DL}}$ are the SINR on subcarrier $k$ in UL and DL, respectively, $z = \Delta f + \varepsilon_D + \tau$, $|S_{k,k'}|^2 = P_{k'}G_{k,k'}$, and $P_{\text{CCI},k}$ is the received CCI power on subcarrier $k$. Note that all parameters belong to the same cell, thus superscripts used earlier to indicate cell index are omitted, and further, $G_{k,k'}^l |H_{k,k'}^l|^2 |C_{k,k'}^l(z)|^2$ is used instead of $\widetilde{G}_{k,k'}^l(\cdot)$.

Classical water-filling approaches have been intensively studied in literature (e.g., in [11, 12] and the references therein). However, in the light of the recent research initiatives on *green radio*, an interesting question is to find a method of throughput maximization while minimizing total power, for which, to the best knowledge of the authors, no closed-form solution exists. Hence, a heuristic algorithm is employed that finds an SINR target assignment and a power assignment, which results in maximum achievable throughput realized with minimum power.

If it is assumed that subcarriers are allocated discrete SINR targets from the target set $\mathbf{\Gamma}$, many ways exist in which these targets can be assigned, such that the same throughput is maintained; however, it is interesting to obtain an assignment which minimizes the total power. The problem of minimizing the total power for a given sum rate $\widetilde{R}$ can be expressed mathematically as given below, assuming that $\overline{p}$ is the maximum power allowed per subcarrier and using each $\overline{\gamma}_k$ corresponds to an $r_k$ belonging to the set of rates, as defined in Section 2:

$$\min \sum_{k=1}^{N_c} P_k \qquad (8)$$

subject to the following constraints:

$$\overline{\gamma}_k \in \mathbf{\Gamma}, \quad \mathbf{\Gamma} = \{0, \widetilde{\gamma}_1, \widetilde{\gamma}_2, \ldots, \widetilde{\gamma}_m\}, \qquad (9)$$

$$0 \leq P_k \leq \overline{p}, \qquad (10)$$

$$\sum_{k=1}^{N_c} r_k = \widetilde{R}. \qquad (11)$$

Now, assuming that there exists an SINR target assignment which fulfills (9), (10), and (11), an important corollary is used, which is proved for CDMA [8] and can be analogously proved for an OFDMA system (proof not shown), *viz.*

**Corollary 1.** *If the subcarriers are arranged at each BS according to the weighted link gains, $G_1|H_1|^2 \geq G_2|H_2|^2 \geq \cdots \geq G_{N_c}|H_{N_c}|^2$, the total power in the cell is minimized for a given throughput if the SINR targets are reassigned such that $\overline{\gamma}_1 \geq \overline{\gamma}_2 \geq \cdots \geq \overline{\gamma}_{N_c}$.*

In other words, while maintaining a given sum rate, minimum total power is used if the subcarriers are ordered according to their link gains (best link gain first) and the SINR targets are reassigned in descending order.

An interesting question now is to obtain the maximum possible rate (or throughput) which can be achieved by the system (i.e., taking a best-effort approach), while at the same time ensuring that this is done with minimum power. This problem is solved heuristically by the GRP, which assigns the highest possible SINR target from the target set to each subcarrier in order to maximize throughput, while power

is minimized according to Corollary 1. The details of the modified GRP derivation can be found in Appendix A, while the pseudocode of the algorithm is shown in Algorithm 1.

### 3.2. Modified OTA-SRR

The OTA-SRR is a scheduling algorithm which jointly allocates rate and power. Zander and Kim introduce the stepwise removal algorithm in [13]. Later in [7], Ginde presents the OTA-SRR which is based on the stepwise removal algorithm, and also includes optimization criteria. OTA-SRR aims to maximize the sum of SINR values of the users in a cellular system. The requirements for this maximization are identified by the OTA, which is then the basis for a linear programming problem, solved by the SRR algorithm. The algorithm starts off with assigning all users maximum SINR target out of a predefined set. Then, the users, which experience maximum interference, are identified and their SINR target is decreased in a step-wise manner until the system satisfies the conditions identified by the OTA. Unlike the GRP, which aims to maximize throughput while minimizing power and hence serves the best-placed users in terms of link gain, the OTA-SRR exhibits fairness in that there is no power minimization constraint. As a consequence, all users are initially assigned maximum rate. Rates are then iteratively reduced based on achieved SINR until the system is in a feasible steady state.

In this paper, the aforementioned scheduling scheme is formulated as a subcarrier, rate, and power allocation algorithm for OFDMA systems. An essential part of this new formulation is the SINR equation. This enabled us to directly apply the existing algorithm constraints and derivations. The modified OTA-SRR is summarized as follows: initially, each user gets a number of subcarriers (depending on the number of users in the cell) with maximum SINR targets, out of a predefined set, assigned to all subcarriers. Under the assumption of a moderately loaded or overloaded system, not all users can support the assigned SINR targets. Iteratively, the subcarriers, which experience maximum interference, are identified, and their SINR target is decreased in a step-wise manner, in an effect adapting the modulation scheme. If the SINR target of a subcarrier is downrated below the minimum value from the target set, the subcarrier is given to a different user from the same BS, such that interference on the subcarrier is minimized. If such user is not found, the subchannel is not used. OTA-SRR is executed until the system reaches feasibility according to the constraints presented in this section.

The algorithm takes into account the interference effects among all subcarriers, thus each subcarrier (out of the total considered in the algorithm, i.e., $BN_c = N$) is given a unique identification (ID) in the range $[1, 2, \ldots, N]$ (i.e., subcarrier one used in cell one has ID 1, subcarrier one in cell two has ID $N_c + 1$, subcarrier two used in cell two has ID $N_c + 2$, etc.). Based on this, the SINR equation given in (5) can be rewritten as

$$\gamma_k = \frac{P_k \widetilde{G}_k}{\sum_{k'=1,\, k' \notin \mathbf{s}}^{N} P_{k'} \widetilde{G}_{k,k'} + n}. \qquad (12)$$

(1) $\bar{\gamma}_k = 0$ and $P_k = \bar{p} \;\forall k$

(2) Compute $P_{\mathrm{CCI},k} \;\forall k$ and $\underbrace{\sum_{k'=1,\, k'\notin \mathbf{s}}^{N_c} |S_{k,k'}|^2 |H_{k,k'}|^2 |C_{k,k'}(z)|^2}_{\text{MAI}} \;\forall k$ in UL

(3) **for** $k = 1$ **to** $N_c$ **do**

    (a) **if** subcarrier $k$ is in UL **then:**

$$\bar{\gamma}_k := \left\{ \max_{\bar{\gamma}_k \in \Gamma}(\bar{\gamma}_k) : \sum_{k'=1}^{k} \frac{\bar{\gamma}_{k'} |C_{k,k'}(z)|^2}{1 + \bar{\gamma}_{k'} |C_{k,k'}(z)|^2} \le 1 - \frac{\bar{\gamma}_k \sum_{k'=1}^{k} (\bar{\gamma}_{k'} |C_{k,k'}(z)|^2 (P_{\mathrm{CCI},k'} + n)/(1 + \bar{\gamma}_{k'} |C_{k,k'}(z)|^2))}{(1 + \bar{\gamma}_k)\bar{p} G_k |H_k|^2 - \bar{\gamma}_k(P_{\mathrm{CCI},k} + n)} \right\}$$

$$P_k = \frac{\bar{\gamma}_k}{(1 + \bar{\gamma}_k) G_k |H_k|^2} \left( \frac{\sum_{k'=1}^{N_c} (\bar{\gamma}_{k'} |C_{k,k'}(z)|^2 (P_{\mathrm{CCI},k'} + n)/(1 + \bar{\gamma}_{k'} |C_{k,k'}(z)|^2))}{1 - \sum_{k'=1}^{N_c} (\bar{\gamma}_{k'} |C_{k,k'}(z)|^2/(1 + \bar{\gamma}_{k'} |C_{k,k'}(z)|^2))} + P_{\mathrm{CCI},k} + n \right)$$

    (b) **if** subcarrier $k$ is in DL **then:**

$$\bar{\gamma}_k := \left\{ \max_{\bar{\gamma}_k \in \Gamma}(\bar{\gamma}_k) : \bar{\gamma}_k \le \left[ \frac{\bar{p} G_k |H_k|^2}{P_{\mathrm{CCI},k} + n} \right] \right\}$$

$$P_k = \frac{\bar{\gamma}_k}{G_k |H_k|^2}(P_{\mathrm{CCI},k} + n)$$

(4) **end**

(5) Update the transmit power, SINR (and respective rate) assignment for all subcarriers

(6) **if** $P_k > \bar{p} \;\forall k$ **then:**

    Block subcarrier $k$

(7) **if** SINR assignment feasible **then:**

    Keep power assignment and SINR assignment

(8) **else**

    go to 2

ALGORITHM 1: Modified GRP.

Note that (12) and (5) differ in their representation only. By dividing the numerator and denominator of the right-hand side of (12) by $\tilde{G}_k$ and transforming it into matrix notation, (12) can be rewritten as

$$(\mathbf{I} - \boldsymbol{\Phi})\mathbf{P} \ge \boldsymbol{\eta}, \tag{13}$$

where $\mathbf{I}$ is the identity matrix, $\boldsymbol{\Phi}$ is the normalized link gain matrix (with dimensions $N \times N$), defined as

$$\Phi_{k,k'} = \frac{\bar{\gamma}_k \tilde{G}_{k,k'}(\cdot)}{\tilde{G}_k}, \tag{14}$$

and $\boldsymbol{\eta}$ is the normalized noise vector, given as

$$\eta_k = \frac{\bar{\gamma}_k n}{\tilde{G}_k}, \tag{15}$$

with $\bar{\gamma}_k \in \Gamma$, for all $k \in N$. The inequality in (13) holds as each subcarrier strives to achieve SINR greater or equal to the target. The OTA constraints on the algorithm are defined based on the properties of $\boldsymbol{\Phi}$ and its dominant eigenvalue $\lambda_1$ (real, positive, and unique, according to the Perron-Frobenius theorem [14]). For $\boldsymbol{\Phi}$, it holds that it is real, nonnegative, and irreducible, that is, the path gains and the SINR targets are real and nonnegative, and the path gains are assumed to be uncorrelated. A solution for the system inequality given in (13) exists, only if the right-hand side of $\mathbf{P} \ge (\mathbf{I} - \boldsymbol{\Phi})^{-1}\boldsymbol{\eta}$ converges. The conditions for convergence of the modified OTA-SRR algorithm are presented in Appendix B and the algorithm is shown in Figure 2.

## 4. SIMULATION MODEL

The simulation model considers an OFDMA-TDD network with a total of 200 uniformly distributed users in a 19-cell region, where each cell has a centrally-located BS. However, a best-effort full-buffer system is in place, which means that all users demand service at all times and the quality of service (QoS) desired by a user corresponds to the maximum data rate it can support. TDD is modeled by assuming a single time slot, where each BS is assigned to either UL or DL, and UL:DL ratios of 1:1, 1:6, and 6:1 are explored. In the case of RTSO, the UL/DL time slot assignment is asynchronous among cells and the assignment of each cell is random with probability depending on the asymmetry ratio studied. When FSA is in place, all cells are synchronously assigned UL or DL with the same probability, thereby modeling symmetric traffic. Here, it should be noted that channel allocation and scheduling are two disjoint processes, so that after each BS has been assigned to either UL or DL, scheduling takes place. A quasistatic model is employed where the link gains between transmitters and receivers remain unchanged for a time slot duration. A BS-MS pair (i.e., a link) is formed based on minimum path loss. The system parameters used in the simulation are shown in Table 1. Note that because of the snapshot nature of the simulation, MSs appear static. However, Doppler frequency offset errors and offset errors due to synchronization are accounted for by using constant offset values. In particular, Doppler frequency offset corresponding to a speed of 30 km/h and 50% synchornization offset are
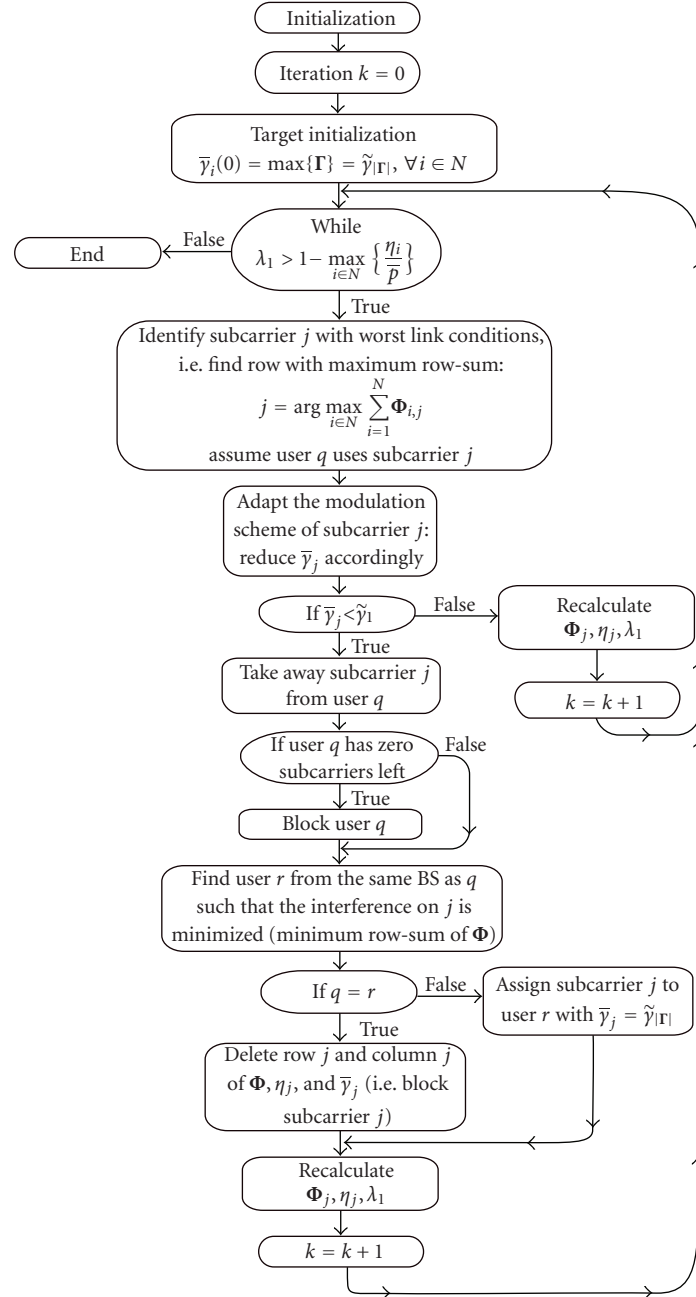
FIGURE 2: Flowchart of the modified OTA-SRR algorithm.

used. The latter value is chosen to reflect a severe interference scenario (e.g., [15] report $\approx 30\%$ offset).

The small-scale fading effects are simulated via a Monte Carlo method [16], which takes into consideration the effects of Doppler shift and time delay. A power delay profile is used corresponding to the specified delay spread in Table 1 [17]. It is assumed that a proper cyclic prefix is in place such that intersymbol interference (ISI) is avoided. The path loss model to account for large-scale fading is chosen accordingly,

[18]—Terrain Category A (suburban), shown as follows:

$$P_{\mathrm{L}} = 20 \log_{10}\left(\frac{4\pi d_0 f}{c}\right) + 10\xi \log_{10}\left(\frac{d}{d_0}\right) + X_\sigma \; [\mathrm{dB}],$$

(16)

where $d_0$ is the reference distance in meters, $f$ is the carrier frequency, $c$ is the speed of light ($3 \times 10^8$ m/s), $\xi$ is the path loss exponent, $d$ is the transmitter-receiver

TABLE 1: Fixed parameters.

| Number of BSs | 19 | Number of MSs | 200 |
|---|---|---|---|
| Cell radius | 500 m | Bandwidth | 100 MHz |
| Number of subcarriers | 2048 | RMS delay spread | 0.27 $\mu$s |
| Carrier frequency | 1.9 GHz | Maximum Doppler frequency | 190 Hz |
| Maximum power per link | 2 W | Freq. offset due to synchronization | 0.5 |

separation distance in meters, and $X_\sigma$ is a zero-mean normally distributed random variable. The path loss in (16) is lower-bounded by the free space path loss [9], $\widetilde{P}_L$, given by

$$\widetilde{P}_L = 20 \log_{10} \left( \frac{4\pi f}{c} \right) + 20 \log_{10}(d) \ \text{[dB]}. \tag{17}$$

Results for a system with NLOS conditions for all TDD interference scenarios (MS $\rightarrow$ BS, BS $\rightarrow$ MS, BS $\rightarrow$ BS, MS $\rightarrow$ MS) are compared against results for an equivalent system where LOS in the case of BS $\rightarrow$ BS interference is assumed (and NLOS for the remaining scenarios). The path loss in the case of LOS is calculated using the free space path loss model, given in (17); and the worst-case scenario is assumed with 100% probability of LOS. Adaptive modulation is achieved with seven different modulation schemes [19] given in Table 2, based on the received SINR for a BER of $10^{-7}$ (necessary for real-time services such as video streaming). The corresponding data rates, $\Upsilon$, are calculated using $\Upsilon = M\Upsilon_{code}/T_s$, where $M$ is the number of bits per symbol, $\Upsilon_{code}$ is the code rate (here, 2/3), and $T_s$ is the symbol time (including cyclic prefix of 20%). Note that the *cross* and *star* constellations are QAM variations in order to ensure robustness to interference, as described in [20, 21], respectively.

## 5. RESULTS AND DISCUSSION

The algorithms implemented in this study are evaluated on the basis of three metrics, *viz spectral efficiency*, *subcarrier utilization*, and *user outage*, described below. *Spectral efficiency* is the achieved system throughput divided by the total bandwidth divided by the number of BSs, *subcarrier utilization* is the number of subcarriers used in the system, divided by the total number of subcarriers (number of subcarriers per BS times the number of BSs), and *user outage* is defined as the users not served (assigned zero subcarriers) as a fraction of the total number of users in the system. All metrics pertain to the whole system, that is, UL and DL combined, unless stated otherwise. In addition, as mentioned in Section 4, a TDD system is simulated assuming a single time slot which is either assigned to UL or DL traffic. This means that for every time slot a different user distribution is analyzed. Since TDD can essentially be characterized as a half-duplex system, this is deemed a sensible approach in order to obtain insightful statistical results on essential system metrics.

The variation of spectral efficiency with asymmetry and LOS conditions for the BSs can be seen in Figures 3(a)

and 3(b) for the modified OTA-SRR and the modified GRP, respectively. A clear trend can be observed for both scheduling schemes. In particular, with an increase in the number of time slots allocated to DL, the spectral efficiency increases and reaches 90% of the theoretical maximum, which is $(\Upsilon_{max} \times N_c \times B/W)/B = \Upsilon_{max}/W_c = 4.44$ bps/Hz/cell, where $W$ is the system bandwidth, $W_c$ is the bandwidth per subcarrier, and $\Upsilon_{max}$ is the maximum data rate per subcarrier (as given in Table 2). Moreover, Figures 3(a) and 3(b) show that LOS conditions among BSs degrade performance significantly. For an asymmetry of 6:1 (UL:DL), the spectral efficiency at the 50th percentile for OTA-SRR and GRP decreases by $\approx$30% and $\approx$50%, respectively. In contrast, the systems employing DL-favored asymmetry are more robust to LOS among BSs. The difference between the spectral efficiency achieved by the NLOS system and the LOS system for an asymmetry of 1:6 (UL:DL) amounts to $\approx$8% and $\approx$6% at the 50th percentile for OTA-SRR and GRP, respectively. This observation is as expected, due to the fact that in DL-favored asymmetries, the occurrence of BS $\rightarrow$ BS interference is significantly limited. It is interesting to note, however, that in terms of spectral efficiency, OTA-SRR is considerably more robust to the detrimental BS $\rightarrow$ BS interference during UL-favored asymmetries than GRP. The algorithms' "robustness" tends to equalize as the asymmetry becomes in favor of DL. The fact that GRP is more sensitive to interference can be explained by its mechanism: GRP identifies the few best-placed users (in terms of path loss) to be served with the highest achievable data rates. With a deterioration in the interference conditions, there is a severe reduction in the number of best-placed users and the data rates that these users can achieve. In contrast, OTA-SRR tries to serve all users, giving each user only the subcarriers that they can utilize. Thus, OTA-SRR adapts to the overall interference and that is why the degradation of performance is not as severe as in the case of GRP.

The outage results shown in Figures 4(a) and 4(b) for OTA-SRR and GRP, respectively, display a similar trend in terms of the comparative performance of the greedy and fair algorithms. Furthermore, the results demonstrate that allocating more resources to DL improves the outage performance and this result is valid for both scheduling algorithms. A comparison between the outage and spectral efficiency results suggests that the relative performance degradation due to LOS is smaller in the case of outage than in the case of spectral efficiency. This is due to employing adaptive modulation, which allows for various SINR levels to be used before discarding a subcarrier. As a consequence, an

TABLE 2: Adaptive modulation parameters for BER of $10^{-7}$.

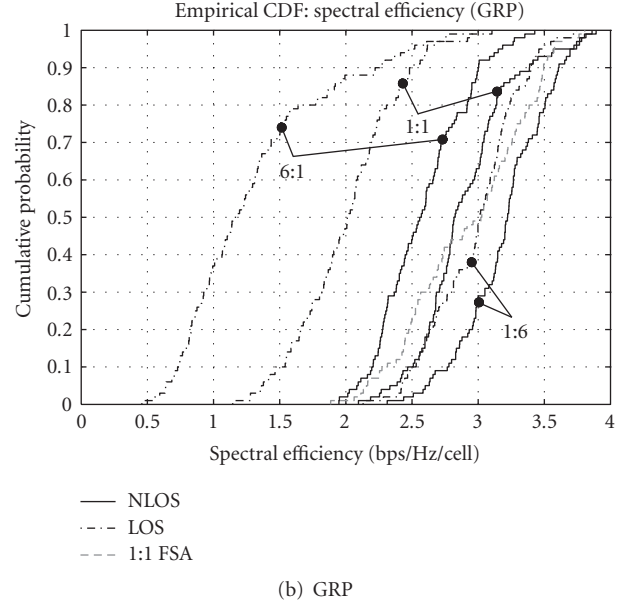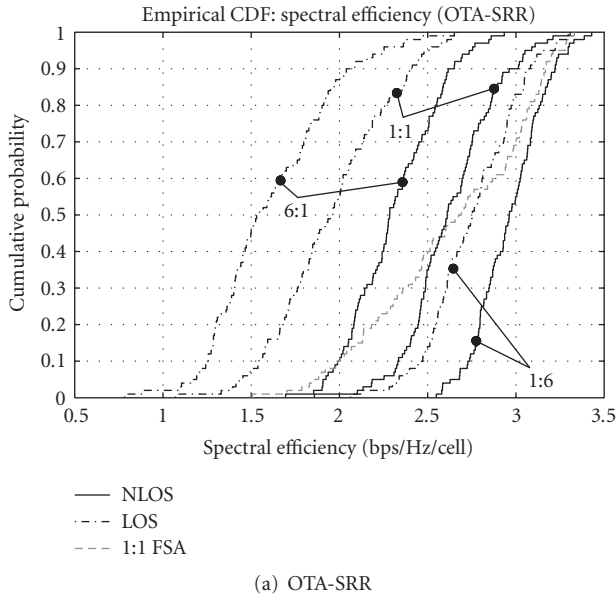| Modulation scheme | 4 QAM | 8 star | 16 QAM | 32 cross | 64 QAM | 128 cross | 256 QAM | |
|---|---|---|---|---|---|---|---|---|
| Data rate | 54.24 | 81.37 | 108.49 | 135.61 | 162.73 | 189.86 | 216.98 | kbps |
| SINR | 9 | 14 | 16 | 19 | 22.2 | 25 | 28.5 | dB |



(a) OTA-SRR

(b) GRP

FIGURE 3: *Spectral efficiency* [bps/Hz/cell] attained by the OTA-SRR and GRP for various UL:DL ratios for cases of LOS and NLOS among BSs. The spectral efficiency is the total throughput in the system divided by the total bandwidth divided by the number of cells.

LOS system could serve approximately the same number of users as an NLOS system (given that all other parameters are the same), but with fewer subcarriers and significantly lower data rates, due to the increased interference. Furthermore, the outage results demonstrate that in the case of OTA-SRR (at the 50th percentile), between ≈57% and ≈83% (at the 50th percentile) of the users are not served, whereas GRP puts between ≈80% and ≈92% of the users into outage. As expected, the fair algorithm offers service to a larger population than the greedy algorithm. It should be noted the outage metric is a relative metric, used for comparison purposes only. The low percentage of served users is due to the severe interference conditions considered.

The overall trends discussed above are also seconded by the subcarrier utilization results presented in Figures 5(a) and 5(b). In addition, it is interesting to note that at the 50th percentile, OTA-SRR utilizes between ≈65% and ≈97% of the available subcarriers, while GRP utilizes between ≈40% and ≈90% of the subcarriers. The fact that OTA-SRR utilizes more subcarriers is not surprising due to the algorithm's fair nature. As previously mentioned, OTA-SRR tries to serve as many users as possible, while utilizing as many subcarriers as possible, while GRP chooses only the "best-placed" users with the "best" channels.

So far, the results have demonstrated superiority in the performance of DL as compared to UL for all considered

metrics. In order to gain insight into the factors that influence the performance of UL and DL, the spectral efficiency performance of UL and DL is studied separately. Results are presented in Figure 6 assuming an UL:DL asymmetry of 1:1 for the following systems, employing RTSO: an OTA-SRR system with NLOS conditions, an OTA-SRR system with LOS conditions among BSs, an ideal OTA-SRR system, and a benchmark system. The *benchmark system* considers neither frequency offset errors nor Doppler errors, that is, it is a purely orthogonal system where the only source of interference is CCI. The resources are allocated randomly at the beginning of each iteration and the SINR per subcarrier is calculated. If the SINR of a particular subcarrier is below the minimum required threshold (Table 2), the subcarrier is discarded and not utilized. If all subcarriers, allocated to a particular user, are discarded, the user is put into outage. The SINR of the subcarriers that can maintain a successful link is used to determine their respective data rates and the spectral efficiency of the system. The *ideal system* is also a purely orthogonal system but, unlike the benchmark system, has resource allocation and adaptive modulation in place. Figure 6 suggests that the spectral efficiency achieved with the benchmark system is the worst, which is as expected because the absence of a scheduling mechanism does not allow for frequency selectivity to be adequately exploited. Moreover, in all cases, DL performs better than UL.
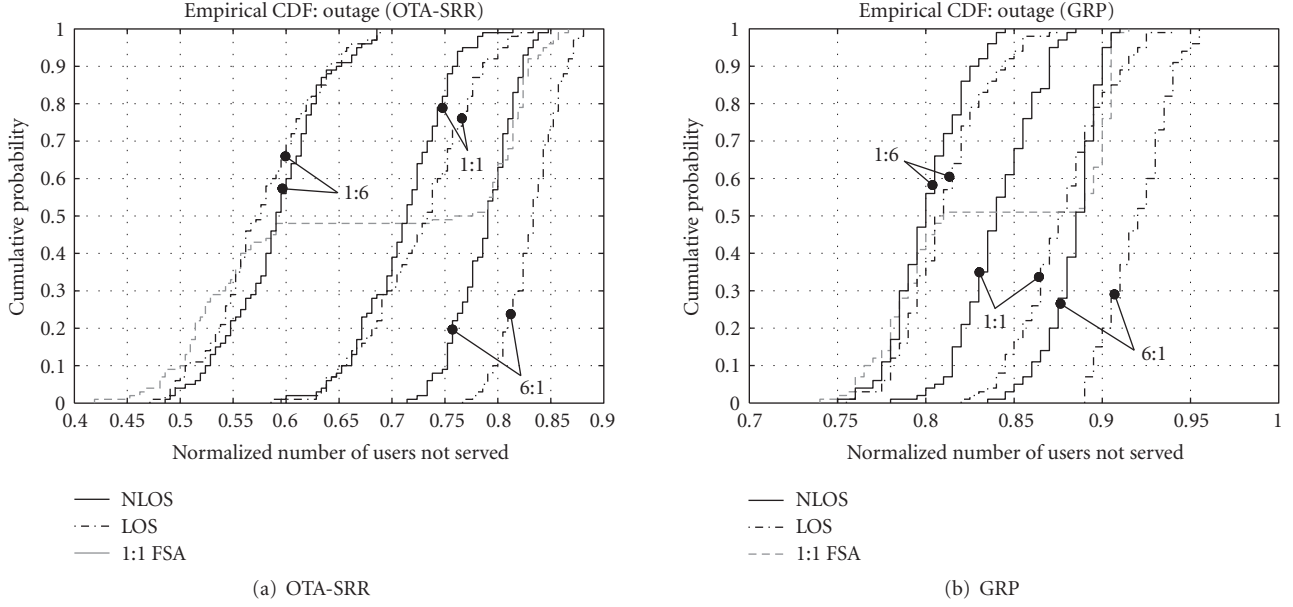
(a) OTA-SRR

(b) GRP

FIGURE 4: *Outage* exhibited by the OTA-SRR and GRP for various UL:DL ratios for cases of LOS and NLOS among BSs. Outage is the ratio of the number of users which are not served to the total number of users in the system.
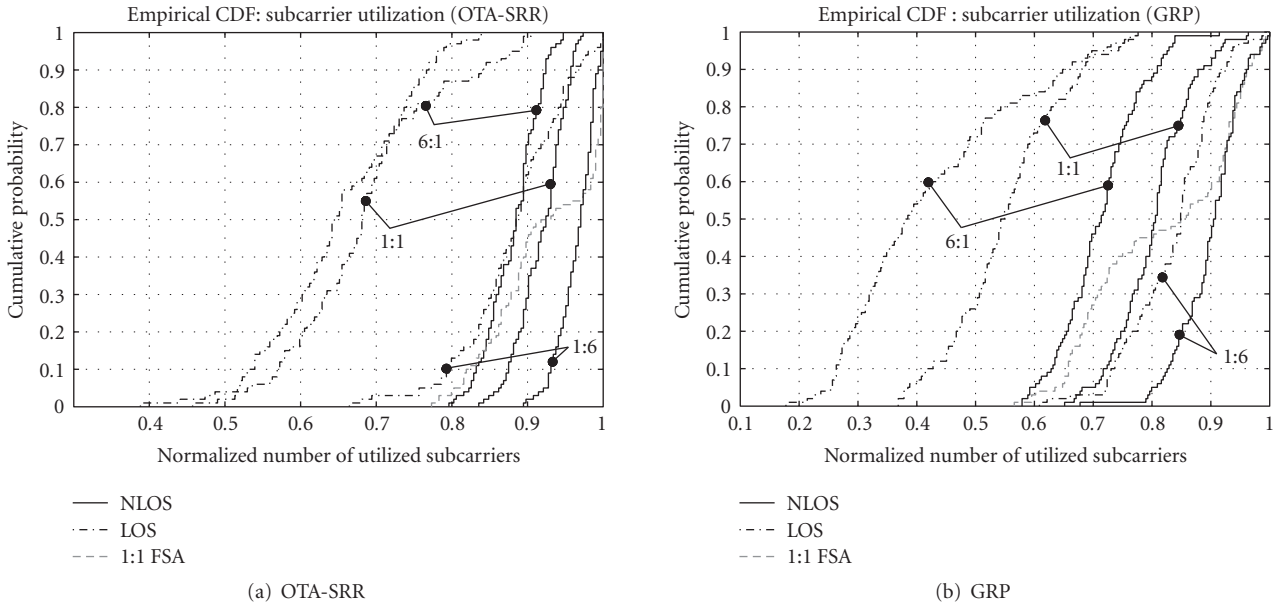


(a) OTA-SRR

(b) GRP

FIGURE 5: *Subcarrier utilization* attained by the OTA-SRR and GRP for various UL:DL ratios for cases of LOS and NLOS among BSs. Subcarrier utilization is the ratio of the number of subcarriers in the system that are used for transmission (i.e., the assigned data rate is greater than (0) to the total number of subcarriers in the system, $N_c \times B$.

This is expected due to the presence of MAI in UL and the lack thereof in DL. In addition, in UL, there is BS → BS and MS → BS interference, while BS → MS and MS → MS interference is characteristic for the DL. For the benchmark system, the difference between UL and DL is about 0.5 bps/Hz/cell at the 50th percentile. In the case of the ideal system, DL only marginally outperforms UL, which is as expected, because frequency selectivity is adequately exploited. However, the difference in UL/DL performance gets more pronounced as LOS conditions for the BSs and offset errors are introduced, that is, in the case of the LOS system and NLOS system, respectively. DL is more favorable in terms of interference, due to the synchronous nature of point-to-multipoint communication and the fact that as the MSs are the receiving units, the detrimental BS → BS LOS effects are not present. Thus, the system
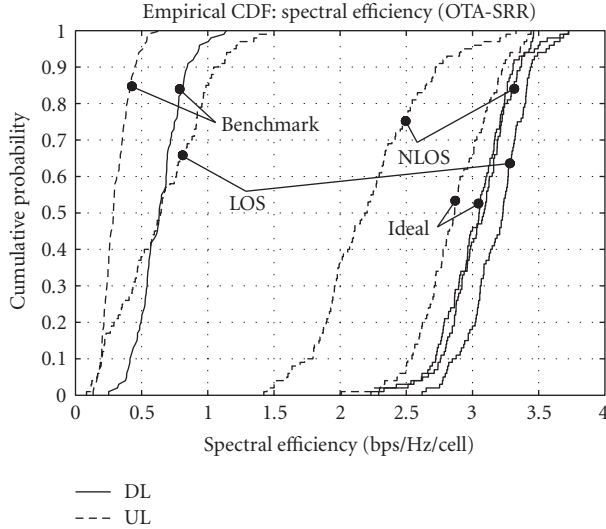
FIGURE 6: UL and DL spectral efficiency attained by OTA-SRR for UL:DL ratio of 1:1.

performance is expected to improve as the asymmetry is shifted in favor of DL, which is in line with the observed results (Figures 3(a) and 3(b)). It is interesting to note, however, that contrary to intuition, DL LOS performs better than DL NLOS. The reason lies in the mechanism of the OTA-SRR algorithm, which operates on all subcarriers (in the cells under consideration) simultaneously. As already discussed, the UL overall performs worse than DL; and this performance gap is enhanced when LOS conditions are considered. Consequently, in an LOS system, the SINR targets of UL subcarriers generally get down rated before the DL subcarriers. As a result, UL subcarriers are discarded before the DL subcarriers. This means that the dimension of the normalized link gain matrix is decreased, which in turn makes the convergence of the algorithm faster. Fast convergence means fewer iterations of step-wise-rate removal, which in turn means fewer-rate removals. As a result, higher data rate per subcarrier is achieved, and, thus, a system is obtained which achieves better spectral efficiency on the DL than an equivalent NLOS system.

In an FSA network, on the other hand, LOS conditions among BS do not cause interference, due to the synchronized UL/DL switching point across the network. Thus, intuitively, it is expected that a symmetric FSA scheme exhibits better performance than an equivalent RTSO system, since it avoids the detrimental BS → BS interference, as well as the MS → MS interference. However, it can be observed that neither of the schemes is strictly better than the other. For instance, assuming OTA-SRR (Figure 3(a)), it can be found that for RTSO, the probability that the spectral efficiency is greater than 2.25 bps/Hz/cell is about 95%, whereas for FSA, this probability is only about 75%. On the other hand, when assuming a spectral efficiency of 3 bps/Hz/cell, it can be found that the same probability for RTSO is 10%, whereas the probability for FSA is 30%. As expected, their medians generally coincide due to the fact that the rate of asymmetry

is the same, and, moreover, the FSA curve spans between the 1:6 (DL-dominated) NLOS and 6:1 (UL-dominated) NLOS RTSO cases. The latter effect is attributed to the shifting of more resources to UL (DL), which creates an interference scenario (MS → BS (BS → MS)) similar to the UL (DL) FSA. Furthermore, it can be observed from all results that the cumulative density function (cdf) graphs for FSA are generally spread out, whereas the cdf graphs for RTSO are comparatively steeper. This means that RTSO offers a more stable and robust QoS, while the QoS offered by the FSA is with larger variation.

An interesting observation can be made with regard to the outage results (Figures 4(a) and 4(b))—the FSA scheme exhibits a "plateau" behavior (bimodal distribution). This can be explained by the presence of MAI in UL, which creates a significant gap between UL and DL performance. Overall, it is observed that the RTSO can successfully exploit interference diversity and thus outperform the FSA scheme in certain scenarios for the same asymmetry. Moreover, shifting more resources in favor of DL achieves better performance than a symmetric FSA system. For example, at a spectral efficiency of 3 bps/Hz/cell, the gain compared to a symmetric UL/DL usage and FSA is about 20% (Figure 3(a)).

With respect to the comparative performance of the two scheduling schemes presented in this paper, the results show a similar trend in the explored metrics. However, GRP, which allocates subcarrier, rate, and power in a greedy manner, achieves only a marginal increase in spectral efficiency at the cost of outage, as compared to the fair OTA-SRR. It is interesting to relate these trends to a similar study done for a CDMA system in [22] with the same cell radius, number of cells, number of users as in the present study. In the case of CDMA, the greedy GRP algorithm as compared to the OTA-SRR scheme displays a twofold increase in terms of total system data rate. At the same time, GRP serves only 30% of the users which are served under the OTA-SRR scheme. Thus, unlike CDMA, in an OFDMA system, the fair OTA-SRR approach is more efficient than the greedy GRP approach.

## 6. CONCLUSIONS

This paper explored UL/DL asymmetry interference aspects in multicellular multiuser OFDMA-TDD systems considering both LOS and NLOS conditions among BSs, when jointly applying channel allocation and user scheduling. The results demonstrated that under RTSO, UL is the performance limiting factor due to unfavorable interference and the hazardous effect of LOS conditions among BSs. It was, furthermore, shown that shifting more resources in DL provides a system robust to these TDD-inherent problems, which is particularly beneficial as future wireless services are expected to be DL-dominated. Such a DL-favored scenario attained up to 90% of the maximum spectral efficiency achievable by the considered network. In addition, for the same asymmetry, RTSO was found to offer a more stable and robust QoS than FSA. The results also demonstrated that, overall, the fair OTA-SRR scheduling algorithm was more robust to the detrimental TDD-specific BS → BS

interference than the greedy GRP algorithm. Furthermore, the fair OTA-SRR served to up to $\approx 20\%$ more users, utilizing up to $\approx 25\%$ more subcarriers, and still achieving spectral efficiencies only marginally lower than those attained by the GRP. Hence, RTSO when combined with OTA-SRR fair scheduling allows the system to retain high spectral efficiency while maintaining fairness in an OFDMA-TDD cellular network with asymmetric traffic.

## APPENDICES

## A. GRP: TRANSMISSION AND POWER CONSTRAINTS

This section treats the derivation of the transmission and power constraints for the GRP algorithm separately for the cases of DL and UL.

### A.1. DL transmission and power constraints

A power minimization problem subject to three constraints was defined in Section 3.1. The first constraint is to choose the SINR targets from the predefined target set $\mathbf{\Gamma}$, the second one is to limit the maximum allowed transmit power per subcarrier to $\overline{p}$, and the third one is a constraint on the sum of SINR targets. Given the first two constraints, GRP aims (1) to maximize the achieved throughput by always assigning the maximum possible SINR target from the target set, and (2) to minimize the total power by using Corollary 1. In order to define the DL GRP algorithm, first, the DL problem statement is formulated and then the power constraint and the throughput maximization condition for the case of DL are derived.

The required power, $P_k$, on a subcarrier $k$ in the DL is given by (A.1), which follows from making $P_k$ the subject of (7). Note that because in DL perfect synchronization is assumed, there is no MAI:

$$P_k = \frac{\overline{\gamma}_k}{G_k |H_k|^2}(P_{\text{CCI},k} + n). \tag{A.1}$$

Hence, the sum of the powers in a cell can be computed as shown below:

$$\sum_{k=1}^{N_c} P_k = \sum_{k=1}^{N_c} \frac{\overline{\gamma}_k}{G_k |H_k|^2}(P_{\text{CCI},k} + n). \tag{A.2}$$

Now the objective function for DL can be expressed as

$$\min\left\{\sum_{k=1}^{N_c} \frac{\overline{\gamma}_k}{G_k |H_k|^2}(P_{\text{CCI},k} + n)\right\}. \tag{A.3}$$

The formulation in (A.3) is subject to a power constraint, which can be expressed mathematically as shown below using (A.1) and limiting the maximum transmit power per subcarrier to $\overline{p}$:

$$\overline{p} \geq \frac{\overline{\gamma}_k}{G_k |H_k|^2}(P_{\text{CCI},k} + n). \tag{A.4}$$

Next, system throughput needs to be maximized. To formulate this for the case of DL, first, the upper bound on $\overline{\gamma}_k$ can be expressed by rearranging (A.4) as follows:

$$\overline{\gamma}_k \leq \frac{\overline{p} G_k |H_k|^2}{P_{\text{CCI},k} + n}. \tag{A.5}$$

This effectively means that for given interference conditions and channel state, the highest SINR target that can be assigned (and achieved) is when the transmit power is maximum. Hence, to maximize throughput, each subcarrier must be assigned the maximum $\overline{\gamma}_k$ from the set $\mathbf{\Gamma}$ which satisfies (A.5). Expressed mathematically, the condition for throughput maximization is

$$\max_{\overline{\gamma}_k \in \mathbf{\Gamma}}\{\overline{\gamma}_k\} \leq \frac{\overline{p} G_k |H_k|^2}{P_{\text{CCI},k} + n}. \tag{A.6}$$

The modified DL GRP algorithm is developed based on (A.4) and (A.6) and is shown in Section 3.1.

### A.2. UL transmission and power constraints

The approach used to formulate the UL GRP algorithm is analogous to the approach used in the case of DL GRP in the previous section.

The required power, $P_k$, on a subcarrier $k$ in UL is derived using (6), where each side of (6) is multiplied by $|C_{k,k}(z)|^2$. For simplicity, the following notation is used:

$$x_k = P_k G_k |H_k|^2 |C_{k,k}(z)|^2, \qquad y_k = P_{\text{CCI},k} + n, \tag{A.7}$$
$$l_k = \overline{\gamma}_k |C_{k,k}(z)|^2,$$

and (6) becomes:

$$l_k = \frac{x_k}{\sum_{k' \notin \mathbf{s}} x_{k'} + y_k}, \tag{A.8}$$

with both $y_k$ and $l_k$ fixed, and $x_k$ to be determined because $P_k$ is of interest. Assuming that $\mathbf{s}$ is composed of only $k$, the above equation can be rewritten as shown below. Note that this is only a simplifying assumption and does not limit the final result to a particular cardinality of $\mathbf{s}$:

$$l_k = \frac{x_k}{\sum_{k'=1}^{N_c} x_{k'} - x_k + y_k}. \tag{A.9}$$

By rearranging the abovementioned data, $x_k$ can be obtained as

$$x_k = \frac{l_k}{1 + l_k}\left(\sum_{k'=1}^{N_c} x_{k'} + y_k\right). \tag{A.10}$$

Next, (A.10) is summed over $k$ and the result is used to substitute $\sum_{k'=1}^{N_c} x_{k'}$ in (A.10) to obtain

$$x_k = \frac{l_k}{1 + l_k}\left(\frac{\sum_{k'=1}^{N_c}(l_{k'} y_{k'}/(1 + l_{k'}))}{1 - \sum_{k'=1}^{N_c}(l_{k'}/(1 + l_{k'}))} + y_k\right). \tag{A.11}$$

Now substitution for $x_k$, $y_k$, and $l_k$ and simplification yield

$$
P_k = \frac{\overline{\gamma}_k}{(1 + \overline{\gamma}_k |C_{k,k}(z)|^2) G_k |H_k|^2}
$$
$$
\times \left( \frac{\sum_{k'=1}^{N_c} (\overline{\gamma}_{k'} |C_{k,k'}(z)|^2 (P_{\mathrm{CCI},k'} + n))/(1 + \overline{\gamma}_{k'} |C_{k,k'}(z)|^2))}{1 - \sum_{k'=1}^{N_c} (\overline{\gamma}_{k'} |C_{k,k'}(z)|^2/(1 + \overline{\gamma}_{k'} |C_{k,k'}(z)|^2))} \right.
$$
$$
\left. + P_{\mathrm{CCI},k} + n \right).
$$
$$(\text{A.12})$$

Note that (A.12) contains $|C_{k,k}(z)|^2$, which is the special case of $|C_{k,k'}(z)|^2$ when $k$ and $k'$ belong to the same user and are the same subcarrier. (Technically, it could also be the case that a subcarrier is reused at a given BS, but this situation is not of interest, as reuse one is assumed here.) Whenever that is the case, there are no errors due to Doppler and no frequency offset errors, and in addition $k - k = 0$, hence $z$ is 0. It can be shown that as $z \to 0$, $|C_{k,k'}(z)|^2 \to 1$ (refer to Appendix C). Therefore, using $|C_{k,k}(z)|^2 = 1$, the required power on a subcarrier $k$ can be expressed as

$$
P_k = \frac{\overline{\gamma}_k}{(1 + \overline{\gamma}_k) G_k |H_k|^2}
$$
$$
\times \left( \frac{\sum_{k'=1}^{N_c} (\overline{\gamma}_{k'} |C_{k,k'}(z)|^2 (P_{\mathrm{CCI},k'} + n))/(1 + \overline{\gamma}_{k'} |C_{k,k'}(z)|^2))}{1 - \sum_{k'=1}^{N_c} (\overline{\gamma}_{k'} |C_{k,k'}(z)|^2/(1 + \overline{\gamma}_{k'} |C_{k,k'}(z)|^2))} \right.
$$
$$
\left. + P_{\mathrm{CCI},k} + n \right).
$$
$$(\text{A.13})$$

Now using (A.13), the objective function for UL is formulated as

$$
\min \left\{ \sum_{k=1}^{N_c} \frac{\overline{\gamma}_k}{(1 + \overline{\gamma}_k) G_k |H_k|^2} \right.
$$
$$
\times \left( \frac{\sum_{k'=1}^{N_c} (\overline{\gamma}_{k'} |C_{k,k'}(z)|^2 (P_{\mathrm{CCI},k'} + n))/(1 + \overline{\gamma}_{k'} |C_{k,k'}(z)|^2))}{1 - \sum_{k'=1}^{N_c} (\overline{\gamma}_{k'} |C_{k,k'}(z)|^2/(1 + \overline{\gamma}_{k'} |C_{k,k'}(z)|^2))} \right.
$$
$$
\left. \left. + P_{\mathrm{CCI},k} + n \right) \right\}.
$$
$$(\text{A.14})$$

As in DL, it is assumed that the maximum transmit power allowed on each subcarrier is $\overline{p}$, however, it should be noted that $\overline{p}$ can be different for UL and DL. Then, the constraint on the UL can be expressed as $P_k \leq \overline{p}$ and using the expression for $P_k$ in (A.13) and rearranging it, the UL power constraint can be expressed as

$$
\sum_{k'=1}^{N_c} \frac{\overline{\gamma}_{k'} |C_{k,k'}(z)|^2}{1 + \overline{\gamma}_{k'} |C_{k,k'}(z)|^2}
$$
$$
\leq 1 - \frac{\overline{\gamma}_k \sum_{k'=1}^{N_c} (\overline{\gamma}_{k'} |C_{k,k'}(z)|^2 (P_{\mathrm{CCI},k'} + n))/(1 + \overline{\gamma}_{k'} |C_{k,k'}(z)|^2))}{(1 + \overline{\gamma}_k) \overline{p} G_k |H_k|^2 - \overline{\gamma}_k (P_{\mathrm{CCI},k} + n)}.
$$
$$(\text{A.15})$$

Now, note that for given $\overline{\gamma}_k$, $G_k$, and $|H_k|^2$, the expression in (A.14) is minimized when $1 - \sum_{k'=1}^{N_c} (\overline{\gamma}_{k'} |C_{k,k'}(z)|^2/(1 + \overline{\gamma}_{k'} |C_{k,k'}(z)|^2))$ is maximized which is equivalent to minimizing the left-hand side of (A.15), that is, $\sum_{k'=1}^{N_c} (\overline{\gamma}_{k'} |C_{k,k'}(z)|^2/(1 + \overline{\gamma}_{k'} |C_{k,k'}(z)|^2))$. This equivalence holds because

$$
\sum_{k'=1}^{N_c} \frac{\overline{\gamma}_{k'} |C_{k,k'}(z)|^2}{1 + \overline{\gamma}_{k'} |C_{k,k'}(z)|^2} < 1,
$$
$$(\text{A.16})$$

due to the fact that $\overline{\gamma}_{k'} |C_{k,k'}(z)|^2$ is always greater than or equal to 0. Hence, the minimization of the left-hand side of (A.15) can be expressed as

$$
\sum_{k'=1}^{N_c} \frac{\overline{\gamma}_{k'} |C_{k,k'}(z)|^2}{1 + \overline{\gamma}_{k'} |C_{k,k'}(z)|^2}
$$
$$
\leq 1 - \max \left\{ \frac{\overline{\gamma}_k \sum_{k'=1}^{N_c} (Z/(1 + \overline{\gamma}_{k'} |C_{k,k'}(z)|^2))}{(1 + \overline{\gamma}_k) \overline{p} G_k |H_k|^2 - \overline{\gamma}_k (P_{\mathrm{CCI},k} + n)} \right\},
$$
$$(\text{A.17})$$

where $Z$ denotes $\overline{\gamma}_{k'} |C_{k,k'}(z)|^2 (P_{\mathrm{CCI},k'} + n)$.

The fraction on the right-hand side of the above inequality is actually maximized when the largest possible $\overline{\gamma}_k$ is chosen from the set $\boldsymbol{\Gamma}$ such that (A.17) is satisfied. Based on (A.15) and (A.17), a rate packing algorithm is developed for the UL, given in Section 3.1. Note that for the special case where all subcarriers in a cell belong to one user, there is no MAI and the UL GRP algorithm is the same as the DL GRP algorithm.

## B. OTA-SRR: CONSTRAINTS AND ALGORITHM CONVERGENCE

This section briefly reviews the OTA constraints and the convergence issues pertaining to the OTA-SRR algorithm [7]. More detailed treatment can be found in [7].

The conditions for convergence of the system equation (13) are outlined below:

$$
(\mathbf{I} - \boldsymbol{\Phi})^{-1} = \mathbf{I} + \boldsymbol{\Phi} + \boldsymbol{\Phi}^2 + \cdots,
$$
$$
(\mathbf{I} + \boldsymbol{\Phi} + \boldsymbol{\Phi}^2 + \cdots)\mathbf{x} = (1 + \lambda + \lambda^2 + \cdots)\mathbf{x},
$$
$$(\text{B.1})$$

where $\mathbf{x}$ is the eigenvector corresponding to the eigenvalue $\lambda$ of $\boldsymbol{\Phi}$. The series in (B.1) converges if and only if $\lambda < 1$ and this holds for any eigenvalue of $\boldsymbol{\Phi}$. Thus, (13) has a solution, when $\lambda_1 < 1$.

In order to determine a feasible set of transmit powers, let $\mathbf{P}_1$ be the eigenvector corresponding to $(1 - \lambda_1)$, the eigenvalue of $(\mathbf{I} - \boldsymbol{\Phi})$. Then, the system in (13) becomes

$$
(1 - \lambda_1)\mathbf{P}_1 \geq \boldsymbol{\eta},
$$

which is equivalent to

$$
\mathbf{P}_1 \geq \frac{\boldsymbol{\eta}}{1 - \lambda_1}.
$$
$$(\text{B.2})$$

If $\mathbf{P}_{\max}$ is the vector of maximum transmit powers, $\mathbf{P}_1$ must satisfy

$$
\mathbf{P}_1 \leq \mathbf{P}_{\max}.
$$
$$(\text{B.3})$$

Thus, based on (B.2) and (B.3), it follows that

$$\mathbf{P}_{\max} \geq \frac{\eta}{1 - \lambda_1}, \tag{B.4}$$

with $0 \leq \lambda_1 \leq 1$. The system constraint can now be expressed by rearranging (B.4) as

$$1 - \lambda_1 \geq \max_{i \in N}\left\{\frac{\eta_i}{p}\right\}. \tag{B.5}$$

The modified OTA-SRR algorithm is illustrated by the flowchart in Figure 2.

## C. DERIVATION OF THE CYCLIC SINC FUNCTION

The following is a derivation of the cyclic sinc (or modified Dirichlet) function, which accounts for the dependence of the interference contribution from subcarrier $k'$ to subcarrier $k$ on the $|k' - k|$.

Based on the IFFT and FFT operations, the received modulation symbol on subcarrier $k$ (without noise), $\mathcal{R}_k$, can be written as

$$\mathcal{R}_k = \frac{1}{N_c} \sum_{i=0}^{N_c-1} \left[ \sum_{k'=0}^{N_c-1} H_{i,k'} S_{k'} \exp\left(\frac{j2\pi ik'}{N_c}\right) \right] \exp\left(\frac{-j2\pi ik}{N_c}\right), \tag{C.1}$$

where $j$ is the imaginary unit, $S_k$ is the transmit symbol on subcarrier $k$, and $H_{i,k}$ is the channel transfer function of subcarrier $k$. If one contributing propagation path is assumed, the channel transfer function can be expressed as

$$\begin{aligned} H_{i,k'} &= \exp(j\phi) \exp\left(\frac{j2\pi i(\varepsilon_D + \omega)}{N_c}\right) \exp\left(\frac{-j2\pi k'\varepsilon_\tau}{N_c}\right) \\ &\equiv H_{k'} \exp\left(\frac{j2\pi i(\varepsilon_D + \omega)}{N_c}\right), \end{aligned} \tag{C.2}$$

where $\varepsilon_\tau$ is the relative propagation delay, and $\phi$ is the phase. After substituting (C.2) into (C.1) and reordering result in

$$\begin{aligned} \mathcal{R}_k &= \frac{1}{N_c} \sum_{i=0}^{N_c-1} \sum_{k'=0}^{N_c-1} H_{k'} \exp\left(\frac{j2\pi i(\varepsilon_D + \omega)}{N_c}\right) S_{k'} \exp\left(\frac{j2\pi i(k'-k)}{N_c}\right) \\ &\equiv \frac{1}{N_c} \sum_{k'=0}^{N_c-1} H_{k'} S_{k'} \underbrace{\left[ \sum_{i=0}^{N_c-1} \exp\left(\frac{j2\pi i(k'-k+\varepsilon_D + \omega)}{N_c}\right) \right]}_{\text{geometric series}}. \end{aligned} \tag{C.3}$$

The geometric series in (C.3) can be simplified. If $2\pi(k' - k + \varepsilon_D + \omega)/N_c = \beta$, the geometric series representation yields

$$\begin{aligned} \sum_{k=0}^{N-1} \exp(j\beta k) &= \frac{1 - \exp(j\beta N)}{1 - \exp(j\beta)} \\ &\equiv \exp\left(\frac{j(N-1)\beta}{2}\right) \frac{\sin(N\beta/2)}{\sin(\beta/2)}. \end{aligned} \tag{C.4}$$

Using the result from (C.4), the cyclic sinc function $C_{k,k'}(k' - k + \varepsilon_D + \omega)$ can be derived as

$$\begin{aligned} C_{k,k'}(k' - k + \varepsilon_D + \omega) &= \frac{1}{N_c} \frac{\sin(\pi(k' - k + \varepsilon_D + \omega))}{\sin(\pi(k' - k + \varepsilon_D + \omega)/N_c)} \\ &\times \exp\left(\frac{j\pi(k'-k+\varepsilon_D+\omega)(N_c-1)}{N_c}\right), \end{aligned} \tag{C.5}$$

such that (C.3) becomes

$$\mathcal{R}_k = \sum_{k'=0}^{N_c-1} H_{k'} S_{k'} C_{k,k'}(k' - k + \varepsilon_D + \omega). \tag{C.6}$$

The received symbol in (C.6) includes both an interference component and a useful component, and can be written in terms of desired signal power and interference power (in Watts) as

$$\begin{aligned} \mathcal{R}_k &= \underbrace{\sum_{k'=0,\,k'\neq k}^{N_c-1} |H_{k,k'}|^2 P_{k'} G_{k,k'} |C_{k,k'}(k' - k + \varepsilon_D + \omega)|^2}_{\text{interference}} \\ &+ \underbrace{|H_k|^2 P_k G_k |C_{k,k}(k - k + \varepsilon_D + \omega)|^2}_{\text{useful signal}}. \end{aligned} \tag{C.7}$$

However, (C.7) models a general case of MAI, which in Section 2 is straightforwardly tailored to account for multiple subcarriers per link and also to account for CCI. It should be noted that Doppler offset and frequency synchronization errors in the desired signal are not considered as perfect synchronization is assumed, hence, the argument of $|C_{k,k}(k - k + \varepsilon_D + \omega)|^2$ is 0. Using (C.5) and noting that for small $\alpha$, $\sin(\alpha) \approx \alpha$, it can be shown that as the argument of $|C_{k,k}(k - k + \varepsilon_D + \omega)|^2$ goes to 0, $|C_{k,k}(k - k + \varepsilon_D + \omega)|^2$ goes to 1. Hence, the useful (desired) signal power per subcarrier, $R_k$, is expressed as

$$R_k = P_k G_k |H_k|^2 \ [\text{W}]. \tag{C.8}$$

## REFERENCES

[1] C. Y. Wong, R. S. Cheng, K. B. Letaief, and R. D. Murch, "Multiuser OFDM with adaptive subcarrier, bit, and power allocation," *IEEE Journal on Selected Areas in Communications*, vol. 17, no. 10, pp. 1747–1758, 1999.

[2] T. Keller and L. Hanzo, "Adaptive modulation techniques for duplex OFDM transmission," *IEEE Transactions on Vehicular Technology*, vol. 49, no. 5, pp. 1893–1906, 2000.

[3] L. Yan, Z. Wenan, and S. Junde, "An adaptive subcarrier, bit and power allocation algorithm for multicell OFDM systems," in *Proceedings of the Canadian Conference on Electrical and Computer Engineering (CCECE '03)*, vol. 3, pp. 1531–1534, Montreal, Canada, May 2003.

[4] H. Rohling and R. Grünheid, "Performance comparison of different multiple access schemes for the downlink of an OFDM communication system," in *Proceedings of the 47th IEEE Vehicular Technology Conference (VTC '97)*, vol. 3, pp. 1365–1369, Phoenix, Ariz, USA, May 1997.

[5] H. Haas and S. McLaughlin, Eds., *Next Generation Mobile Access Technologies: Implementing TDD*, Cambridge University Press, Cambridge, UK, 2008.

[6] H. Haas, P. K. Jain, and B. Wegmann, "Capacity improvement through random timeslot opposing (RTO) algorithm in cellular TDD systems with asymmetric channel utilisation," in *Proceedings of the 14th International Symposium on Personal, Indoor and Mobile Radio Communications (PIMRC '03)*, vol. 2, pp. 1790–1794, Beijing, China, September 2003.

[7] S. Ginde, *A game-theoretic analysis of link adaptation in cellular radio networks*, M.S. thesis, Virginica Polytechnic Institute and State University, Blacksburg, Va, USA, May 2004.

[8] F. Berggren and S.-L. Kim, "Energy-efficient control of rate and power in DS-CDMA systems," *IEEE Transactions on Wireless Communications*, vol. 3, no. 3, pp. 725–733, 2004.

[9] T. S. Rappaport, *Wireless Communications: Principles and Practice*, Prentice Hall PTR, Upper Saddle River, NJ, USA, 2nd edition, 2001.

[10] IST-2003-507581 WINNER, "D1.3 v1.0 Final Usage Scenarios," June 2005, http://www.ist-winner.org/deliverables_older.html.

[11] W. Yu, G. Ginis, and J. M. Cioffi, "An adaptive multiuser power control algorithm for VDSL," in *Proceedings of the Global Telecommunications Conference (GLOBECOM '01)*, vol. 1, pp. 394–398, San Antonio, Tex, USA, November 2001.

[12] G. Scutari, D. P. Palomar, and S. Barbarossa, "Asynchronous iterative waterfilling for Gaussian frequency-selective interference channels: a unified framework," in *Proceedings of the Information Theory and Applications Workshop (ITA '07)*, pp. 349–358, Lake Tahoe, Calif, USA, September 2007.

[13] J. Zander and S.-L. Kim, *Radio Resource Management for Wireless Networks*, Artech House, Boston, Mass, USA, 2001.

[14] F. R. Gantmacher, *Matrix Theory*, vol. 2, Chelsea, New York, NY, USA, 1974.

[15] M. Speth, S. A. Fechtel, G. Fock, and H. Meyr, "Optimum receiver design for wireless broad-band systems using OFDM. I," *IEEE Transactions on Communications*, vol. 47, no. 11, pp. 1668–1677, 1999.

[16] P. Höher, "A statistical discrete-time model for the WSSUS multipath channel," *IEEE Transactions on Vehicular Technology*, vol. 41, no. 4, pp. 461–468, 1992.

[17] J. Medbo and P. Schramm, "Channel Models for HIPERLAN 2," ETSI/BRAN document no. 3ERIO85B, 1998., September 2006, http://www.etsi.org/.

[18] V. Erceg, L. J. Greenstein, S. Y. Tjandra, et al., "An empirically based path loss model for wireless channels in suburban environments," *IEEE Journal on Selected Areas in Communications*, vol. 17, no. 7, pp. 1205–1211, 1999.

[19] K. J. Hole, H. Holm, and G. E. Øien, "Adaptive multidimensional coded modulation over flat fading channels," *IEEE Journal on Selected Areas in Communications*, vol. 18, no. 7, pp. 1153–1158, 2000.

[20] W. T. Webb, L. Hanzo, and R. Steele, "Bandwidth-efficient QAM schemes for Rayleigh fading channels," in *Proceedings of the 5th International Conference on Radio Receivers and Associated Systems*, pp. 139–142, Cambridge, UK, July 1990.

[21] G. Forney Jr., R. Gallager, G. Lang, F. Longstaff, and S. Qureshi, "Efficient modulation for band-limited channels," *IEEE Journal on Selected Areas in Communications*, vol. 2, no. 5, pp. 632–647, 1984.

[22] E. Foutekova, P. Agyapong, B. Ghimire, H. Venkataraman, and H. Haas, "Scheduling in cellular CDMA-TDD networks," in *proceedings of the 64th IEEE Vehicular Technology Conference (VTC '06)*, pp. 727–731, Montreal, Canada, September 2006.